Modal Analysis – Prof. Arcanjo Lenzi

Lucas Schroeder – Mar. 25th, 2021

Exercise List - 5

EXPERIMENTAL MODAL ANALYSIS

The objective of this work is to study a real case of modal analysis using the experimental results for a beam, obtained using impact hammer. The beam, shown in Figure 1, is made of steel with $\rho = 7880\ kg/m^3$, and has length $L = 0.8\ m$, width $w = 50\ mm$ and height of $h = 5\ mm$.

Figure 1 - Experimental setup

This beam is simply supported at both ends, and have an experimental mesh with 34 Degrees of Freedom (DoF) shown in Figure 2. To input force, a hammer was used at every DoF in the z direction, with the measurement being made with a uniaxial accelerometer at DoF 2, also in the z direction Figure 9.

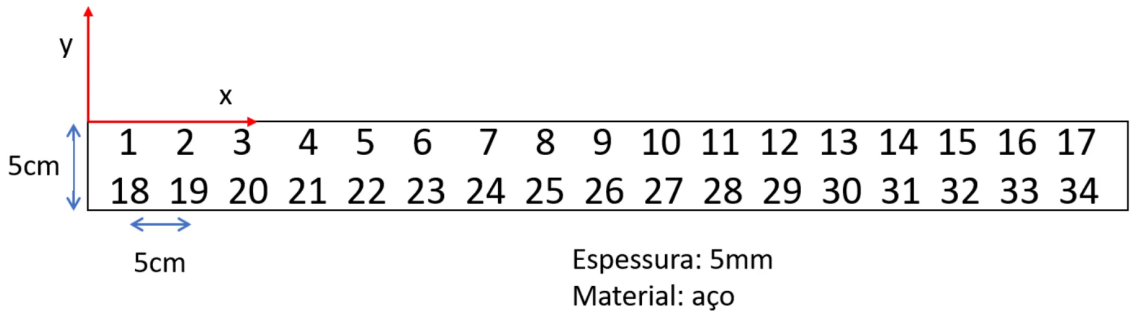

Figure 2 - Degrees of Freedom (DoF) location diagram.

Figure 3 - Response accelerometer at DoF 2.

Using the Stabilization method, the natural frequencies detected were $f_n = [17.212, 68.840, 118.878, 155.391, 226.395, 265.219, 235.230, 362.805, 414.118, 567.539, 602.292, 643.435, 707.200, 740.567, 820.439, 880.725, 943.641]\ Hz$.

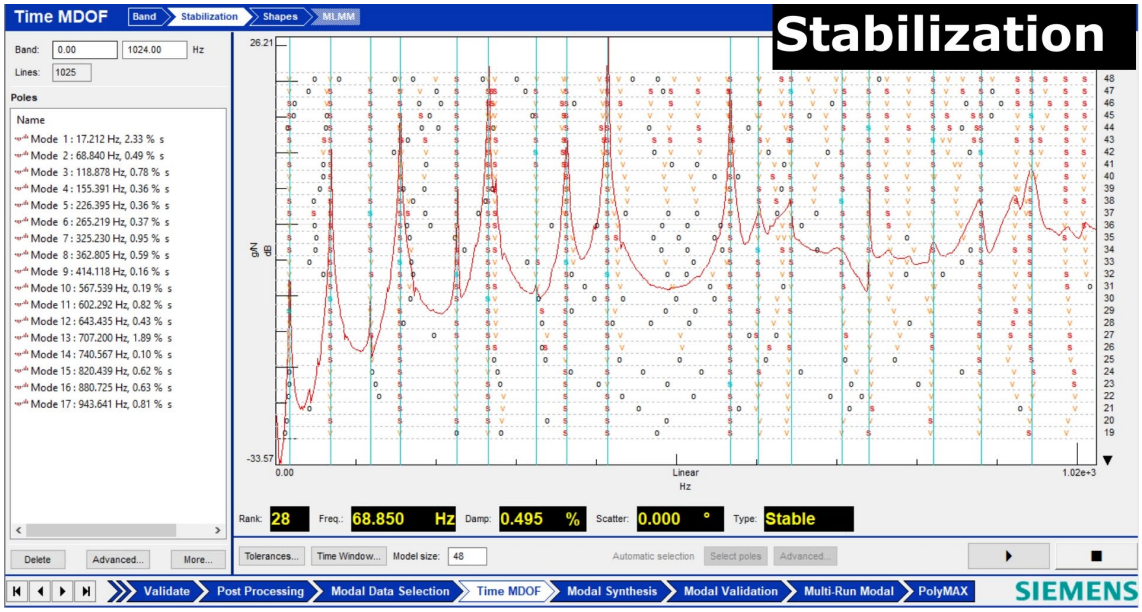

1

Plot the first four modes from the experimental FRF.

To find the mode shapes, we need to find the Nyquist diameters. First, we found the peaks and their respective frequencies ω_n. Then, we found the diameter ${}_n\mathrm{D}_{jk} = (|MX| + |MN|)$ of the Nyquist plot using the maximum MX and minimum MN of the real part of receptance $H_{jk}(\omega)$ around ω_n. We also note the frequencies where the maximum and minimum occurs, so we can calculate the half-power bandwidth and the damping parameter η_n associated to that mode n. Knowing this, we can finally calculate the modal constant using

$$ {}_nA_{jk} = (|MX| + |MN|) f_n^2 \eta_n. \qquad \text{Eq. 1}$$

By definition, modal constants are the product of two mass-normalized components of the mode shapes

$$ {}_nA_{jk} = {}_n\Phi_j \, {}_n\Phi_k. \qquad \text{Eq. 2}$$

So, for the point response of DoF 2, the first component of the n^{th} mode shape is

$$ \left| {}_n\Phi_2 \right| = \sqrt{{}_nA_{22}}. \qquad \text{Eq. 3}$$

From Eq. 2, we can write the components of the n^{th} mode shape, for an input force at DoF 1 and response at DoF 1 through j

$$ \begin{Bmatrix} {}_n\Phi_1 \\ {}_n\Phi_2 \\ \vdots \\ {}_n\Phi_j \end{Bmatrix} = \frac{1}{{}_n\Phi_2} \begin{Bmatrix} {}_nA_{21} \\ {}_nA_{22} \\ \vdots \\ {}_nA_{2k} \end{Bmatrix}. \qquad \text{Eq. 4}$$

This procedure resulted in the following mode shapes:

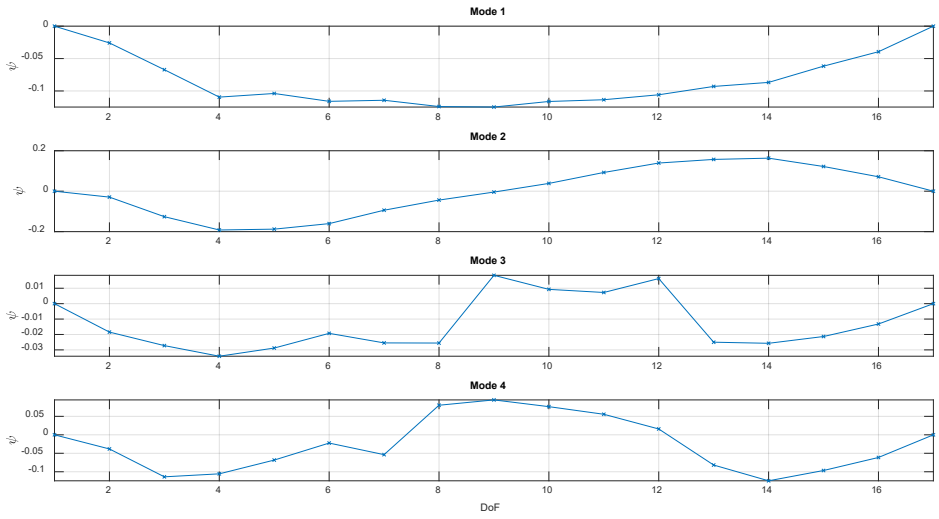

2

Find the type of damping (hysteretic or viscous)

By plotting the inverse receptance $H_{jk}^{-1}(\omega)$ we may infer the type of damping by looking at how its real and imaginary part behave near each resonant frequency. The real part is expected to cross the line $y = 0$ with a negative slope at $\omega = \omega_r$. However, the imaginary part may have two distinct behaviors at $\omega = \omega_r$: it may be constant with respect to ω, indication hysteretic damping or it may have a positive slope, indicating viscous damping.

A clear tendency could be seen, and Figure 4 shows an example of how the inverse receptance behaves near every resonant frequency, and by this we are able to affirm that the best model of damping for this structure is the viscous model.

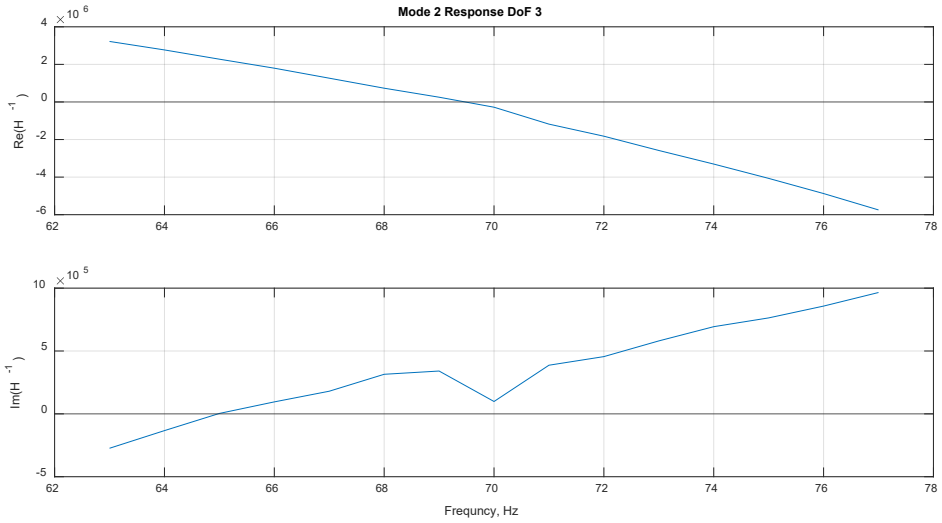

Figure 4 - Real and imaginary part of inverse receptance.

3

Adjust the stiffness of the modes from the 4th mode onward using the concept of Residuals. Compare the regenerated driving point FRF with the measured one.

When we don't use every mode to compute the FRF with the modal constants, we are neglecting the effects of higher or lower modes. To account for that, we may use the Residuals technique to include account for the stiffness and mass of other modes using

$$H_{jk}(\omega) \cong -\frac{1}{\omega^2 M_{jk}^R} + \sum_{r=m_1}^{m_2} \left(\frac{{}_rA_{jk}}{\omega_r^2 - \omega^2 + j\eta_r\omega_r^2} \right) + \frac{1}{K_{jk}^R}. \qquad \text{Eq. 5}$$

In this example, we used only the first four modes and to regenerate the FRF and applied a residual stiffness of $K_{jk}^R = 1 \cdot 10^8\ N/m$ and the results are shown in Figure 5.

Figure 5 - Regenerated FRF with residual stiffness.

4

Adjust a circle into the second mode, as suggested by Nuno Maia, for the FRF measured with a shaker. Compare it with the one obtained with the impact hammer measurements.

We know that the Nyquist plot for each mode should be a circle, so we can use the experimental data to fit one and reduce experimental errors. We are going to use the results obtained with a shaker to fit circles to the second mode of each FRF, and will use the diameters to calculate each modal constant, as per Eq. 1 trough Eq. 4.

First, we select the point around the second resonant frequency for each FRF, then we use V. Pratt's (1987) technique of direct least-squares fitting to find each circle diameter (shown in Figure 7). This resulted in a fairly good result, as shown in Figure 6.

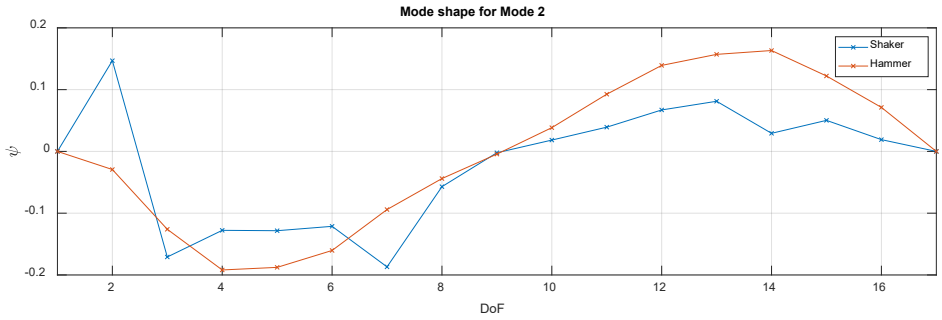

Figure 6 - Second mode shape obtained with shaker and impact hammer.

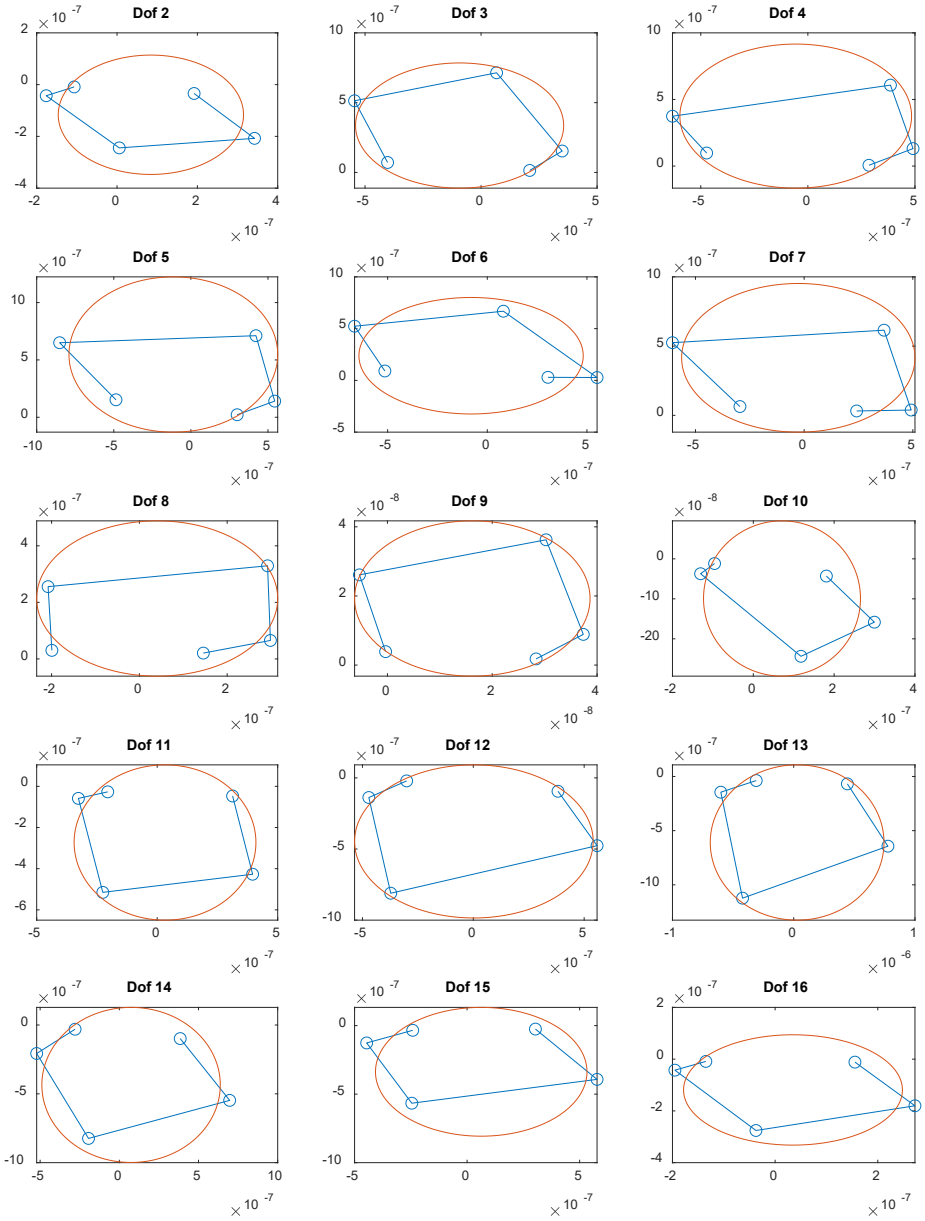

Figure 7 - Circle fit for the second mode for each FRF, with input in DoF 2 and output in DoF 2 to 16.

5

The first four flexing modes shapes may be calculated using

$$H_{jk}(\omega) = \frac{X_j}{F_k} = \sum_{r=1}^{\infty} \frac{{}_r\Phi_j \; {}_r\Phi_k}{\omega_r^2 - \omega + j\eta_r\omega_r^2}, \qquad \text{Eq. 6}$$

where

$$ {}_r\Phi_k = \sqrt{\frac{2}{m}} \sin \frac{r\pi x_k}{L} \qquad \text{Eq. 7} $$

is the k^{th} element of the mass-normalized eigenvector $\{\Phi\}_n$ associated to the eigenvalue ω_n^2, r is the mode number, and x_k is the position of the k^{th} experimental DoF.

$$ \omega_r = r^2\pi^2 \sqrt{\frac{EI}{mL^3}} \qquad \text{Eq. 8} $$

We can use these results to compare with the experimental data. Below we show the mode shapes obtained.

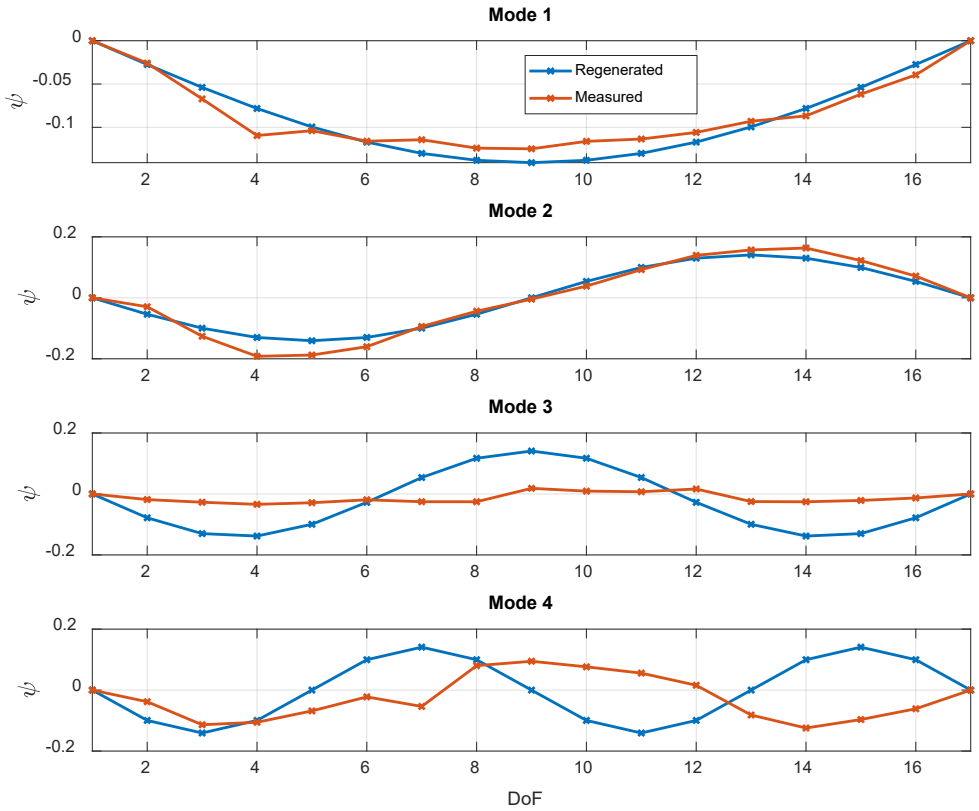

Now, we can compare the measured and the analytical results for two arbitrary points in the structure, chosen to be DoF 2 and 13. The results are shown below.

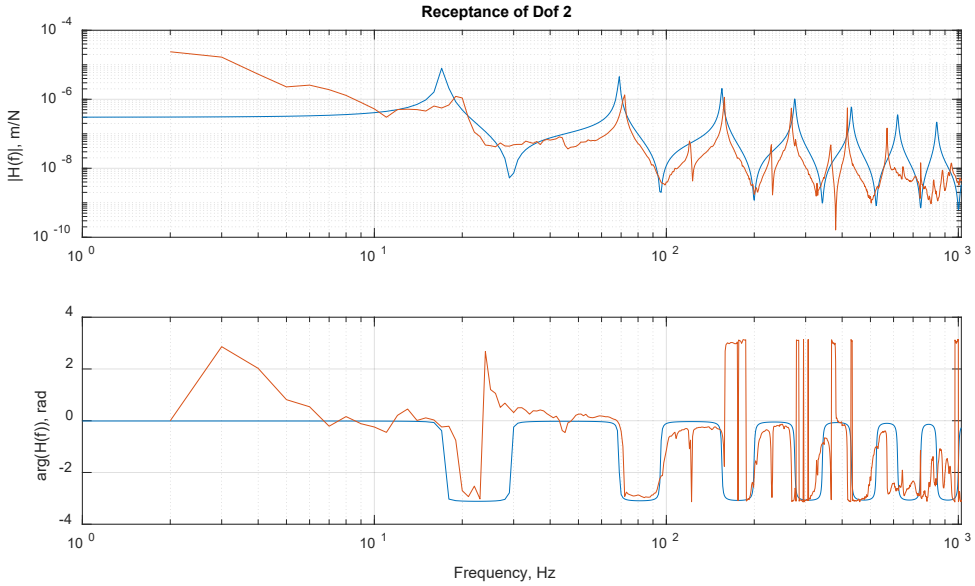

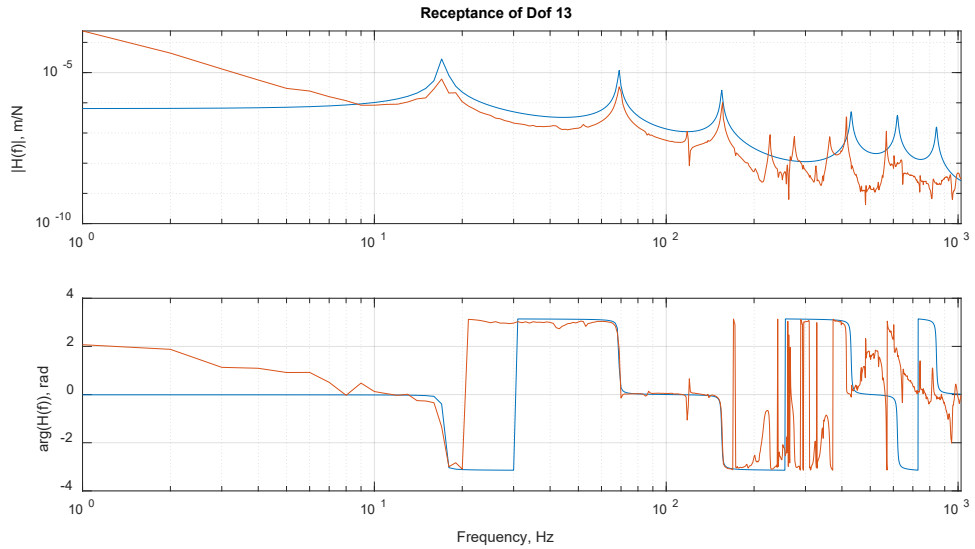

6

Using the analytical results above, calculate the Modal Assurance Criteria (MAC) of the first four flexing mode shapes.

MAC is used to find the correlation between the theoretical and experimental mode shapes, and determine if we are measuring the same things. This is calculated using

$$MAC(A,X) = \frac{|\{\Psi_X\}^T\{\Psi_A\}|^2}{(\{\Psi_X\}^T\{\Psi_X\})(\{\Psi_A\}^T\{\Psi_A\})}. \qquad \text{Eq. 9}$$

Which was implemented in code using:

```
407     %% 6 Compute the Modal Assurance Criteria (MAC) of the first four flexing mode shapes
408     % Phi(j,r) -> % rPhi_j, mode shape for dof j and mode r
409 -   for mode_a = 1:4
410 -       for mode_ex = 1:4
411 -           MAC(mode_a,mode_ex) = (Phi(1:17,mode_ex).'*Phi_anlt(1:17,mode_a))^2/...
412                                   (Phi(1:17,mode_ex).'*Phi(1:17,mode_ex))*(Phi_anlt(1:17,mode_a).'*Phi_anlt(1:17,mode_a));
413 -       end
414 -   end
```

The results for the first 4 modes, both analytical and experimental, are show below.

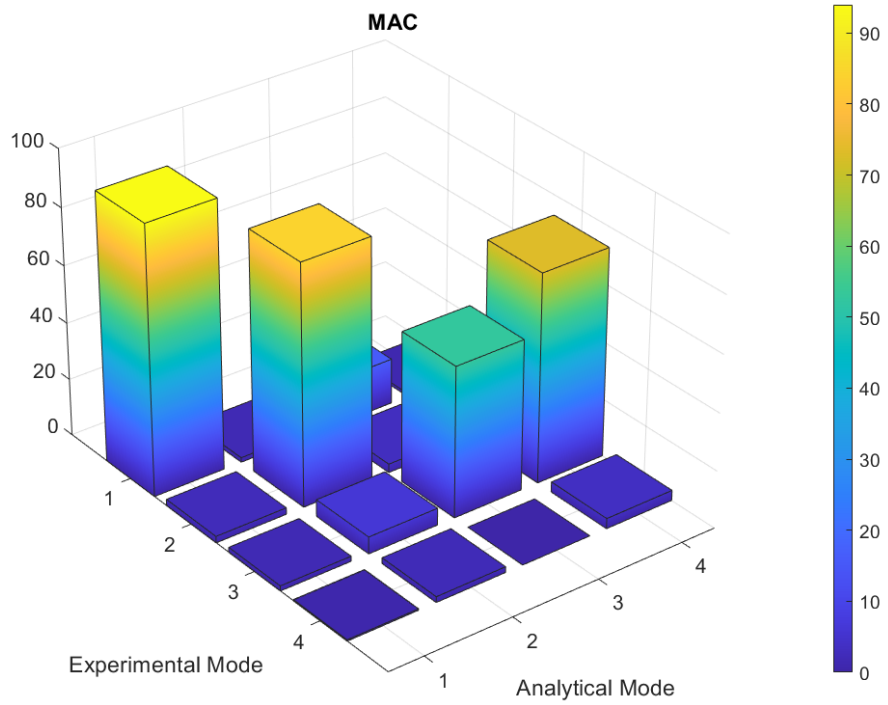

This give us confidence the first two modes are correspondents, since they have same frequency and mode shape. However, the third experimental mode could have another origin that the beam model do not account for.

7

Design a Dynamic Vibration Absorber (DVA) to control the second flexing mode, Then, find the new FRF and compare with the previous one.

The DVA is a mass-spring-damper system, and its receptance is given by

$$H_{DVA}(\omega) = \frac{X_j(\omega)}{F_j(\omega)} = \frac{k - m\omega^2 + j\omega c}{(-m\omega^2)(k + j\omega c)}, \qquad \text{Eq. 10}$$

where k is the spring stiffness (N/m), m is the DVA's mass (kg) and c is its damping (N/(m/s)), as shown in the figure bellow.

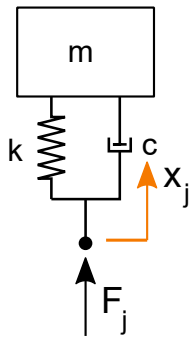

When the DVA is attached to the j^{th} DoF of our beam, we can use the superposition principle for linear time-invariant systems to find the new receptance $H'_{qi}(\omega)$ between input force at DoF i and the response at another arbitrary DoF q, as illustrated below.

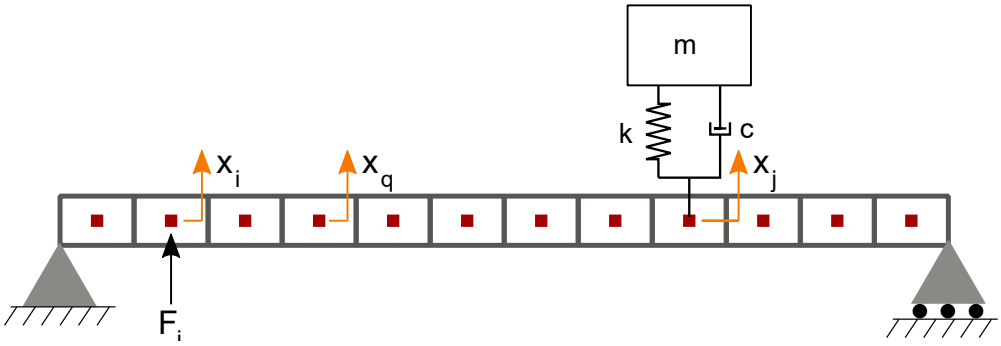

First, let's compute the real displacement of DoF j by summing the contribuition of force F_i and the DVA, then finding the real FRF H'_{ji} between Dof j and i:

$$X'_j(\omega) = H_{ji}F_i - H_{jj}F_j = H_{ji}F_i - H_{jj}\frac{X'_j}{H_{DVA}} \quad \Rightarrow \quad H'_{ji} = \frac{X'_j}{F_i} = \frac{H_{ji}}{\left(1 + \frac{H_{jj}}{H_{DVA}}\right)} \quad \text{Eq. 11}$$

where $H_{ij}(\omega)$ is the beam's receptance between i and j.

Using the same reasoning, let's compute the real displacement of DoF q by summing the contribuition of force F_i and the DVA, noting that the DVA's force F_j due to the displacement X'_j can be computed using Eq. 10, leading to:

$$X'_q(\omega) = H_{qi}F_i - H_{qj}F_j = H_{qi}F_i - H_{qj}\frac{X'_j}{H_{DVA}}. \quad \text{Eq. 12}$$

Now, substituting X'_j by Eq. 11 we have

$$X'_q(\omega) = H_{qi}F_i - H_{qj}\frac{H'_{ji}F_i}{H_{DVA}} = F_i\left(H_{qi} - \frac{H_{qj}H_{ji}}{H_{DVA} + H_{jj}}\right). \quad \text{Eq. 13}$$

And finally, the new receptance between any arbitrary DoF q and i, when an DVA is placed at DoF j is:

$$H'_{qi}(\omega) = \frac{X'_q}{F_i} = H_{qi} - \frac{H_{qj}H_{ji}}{H_{DVA} + H_{jj}}. \quad \text{Eq. 14}$$

Now we should choose the k, m and c parameters of the DVA as well as the position where it should be installed. By inspection of the second mode shape, the bigest displacements, ocour at the DoF 5, 13 22 and 30, so we will install the DVA at DoF $j = 5$. Also, we must tune it to have the smallest receptance (small displacement for a given force) at the frequency of the second mode, which is $f_2 = 68.5\ Hz$, so the ratio on the RHS of Eq. 14 is large and $H'_{qi}(\omega_2)$ decrease.

For this, we chose $k = 370\ kN/m$, $m = 2\ kg$ and $c = 200\ N/(m/s)$, which gives a DVA receptance suited for our purpouses, as shown in Figure 8.

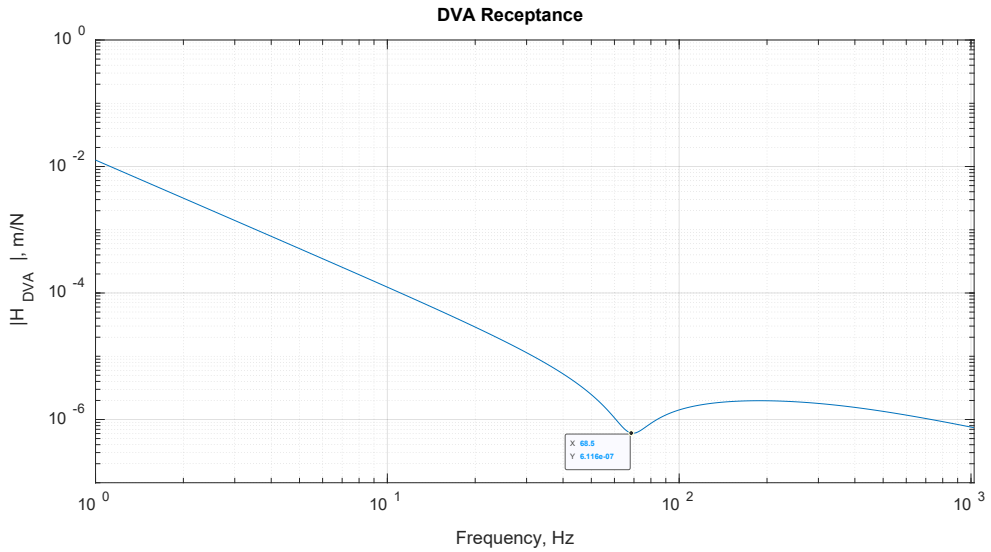

Figure 8 - Dynamic Vibration Absorber receptance curve.

Applying Eq. 14 and comparing $H'_{qi}(\omega)$ with the original FRF H_{qi}, we have a significant reduction of the amplitude of the second mode. For the response at DoF $q = 2$ to a force at DoF $i = 2$, accounting for DVA at DoF $j = 5$ we have a reduction of approximately 10 times in $f = 68.5\ Hz$, as shown in Figure 9.

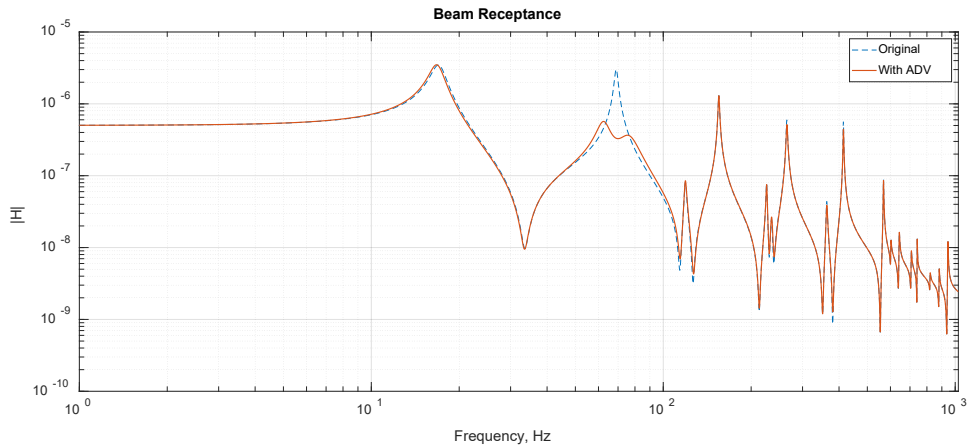

Figure 9 – Receptance for response at DoF $q = 2$ to a force at DoF $i = 2$, accounting for DVA at DoF $j = 5$.